

RAID: Randomized Adversarial-Input Detection for Neural Networks

Hasan Ferit Eniser
MPI-SWS, Germany
hfeniser@mpi-sws.org

Maria Christakis
MPI-SWS, Germany
maria@mpi-sws.org

Valentin Wüstholtz
ConsensSys/MythX, Germany
valentin.wustholz@consenssys.net

ABSTRACT

In recent years, neural networks have become the default choice for image classification and many other learning tasks, even though they are vulnerable to so-called adversarial attacks. To increase their robustness against these attacks, there have emerged numerous detection mechanisms that aim to automatically determine if an input is adversarial. However, state-of-the-art detection mechanisms either rely on being tuned for each type of attack, or they do not generalize across different attack types. To alleviate these issues, we propose a novel technique for adversarial-image detection, RAID, that trains a secondary classifier to identify differences in neuron activation values between benign and adversarial inputs. Our technique is both more reliable and more effective than the state of the art when evaluated against six popular attacks. Moreover, a straightforward extension of RAID increases its robustness against detection-aware adversaries without affecting its effectiveness.

1 INTRODUCTION

There is no doubt that neural networks are becoming rapidly and increasingly prevalent. Their success has been particularly impressive for the task of accurately recognizing patterns and classifying images [57], on which we focus here. Even though such networks are able to achieve very high accuracy for “normal” (i.e., benign) images, they may be tricked by adversaries into providing wrong classifications. More specifically, given a correctly classified image, an adversary may perturb it slightly—*typically almost unnoticeably according to human perception*—to generate an image that is classified differently. Such images are referred to as *adversarial* [58] and pose a serious threat to emerging applications of machine learning, such as autonomous driving [18, 44].

To protect neural networks against adversarial attacks, there have emerged numerous *defense* mechanisms that aim to correctly classify adversarial inputs. However, most of these defenses have not been found effective in preventing adversarial images from being misclassified [9]. As a result, the research community has also focused on automated *detection* of adversarial images, that is, on devising mechanisms for detecting whether an input to a neural network is adversarial (see [11] for examples).

Adversarial-image detection. In the context of adversarial-image detection, some state-of-the-art detection mechanisms are classifier based, that is, they train a secondary classifier for determining whether inputs of a neural network are adversarial. A recent, notable example is SADL [29], an approach that relies on

the observation that “surprising” inputs are more likely to be adversarial. Depending on the surprise measure, the effectiveness of this approach relies on tuning its hyper-parameters, namely which neurons are used to measure surprise, for each type of attack. However, in practice, detection mechanisms are typically unaware of the types of incoming attacks.

In terms of classifier-free detection mechanisms, a novel example is mMutant [60], which assumes adversarial images to be more “sensitive” than normal ones. More specifically, the assumption is that the classification outcome for adversarial inputs is more likely to change when performing minor mutations to the neural network. However, this assumption does not generalize to adversarial inputs with a high prediction confidence, that is, inputs for which the neural network provides a wrong classification with high confidence.

Our approach. To alleviate these issues, we present a new adversarial-image detection technique, called RAID. Our technique is based on teaching a secondary classifier to recognize differences in neuron activation values between adversarial and normal inputs. We show that the effectiveness of RAID is stable with respect to its hyper-parameters across a wide range of adversarial attacks. RAID consistently outperforms SADL and mMutant on these attacks by up to 88%. Moreover, in contrast to these techniques, there exists a simple extension to RAID that increases its robustness against detection-aware adversaries without affecting its effectiveness.

Contributions. Our paper makes the following contributions:

- (1) We present a simple, yet very effective, adversarial-image detection technique for neural networks.
- (2) We extend our technique to increase its robustness against stronger adversaries that can tailor their attacks to specific detection mechanisms.
- (3) We implement our approach and make the implementation publicly available.
- (4) We extensively evaluate our approach and compare it with three state-of-the-art detection techniques.

Outline. The next section provides background on different types of adversaries and attacks. Sect. 3 explains our adversarial-image detection approach. We present our experimental evaluation in Sect. 4, discuss related work in Sect. 5, and conclude in Sect. 6.

2 BACKGROUND

In this section, we give a short overview of threat models and adversarial attacks.

2.1 Threat Models

A *threat model* describes the conditions under which a detection mechanism is designed to work. Consequently, the threat model is necessary for assessing the effectiveness of a detector [9].

Adversarial attacks are typically categorized according to two main threat models: (1) *white-box* attacks, where the adversary has perfect knowledge of the neural network including, for example, its architecture and parameters, and (2) *black-box* attacks, which generate adversarial examples without any internal information about the neural network. In this work, we consider the stronger white-box threat model although our technique is also applicable against black-box attacks. White-box adversaries come in two capacities, namely static and adaptive.

Static adversaries. A *static adversary* is an attacker that is unaware of any detection mechanism protecting a network model against adversarial attacks. A static adversary makes use of existing white-box attacks to generate adversarial examples but does not tailor these attacks to breach any specific detection mechanism.

Adaptive adversaries. An *adaptive adversary* is an attacker that is aware of the detection mechanism protecting a network model, if any. Such an adversary also has knowledge of internal parameters of the detection mechanism. As a result, it may adapt the adversarial attacks it generates to breach the particular detection mechanism that is in place. Adaptive adversaries are clearly more powerful than static ones.

In this paper, we evaluate our approach as well as three state-of-the-art adversarial-image detection techniques on several static adversaries. We also extend our approach to adaptive adversaries and reason about its effectiveness.

2.2 Adversarial Attacks

In the context of deep learning, adversarial examples are generally defined as inputs to a neural network that are specifically crafted to trick it into making a wrong prediction [9]. Practically, such examples are generated by slightly distorting correctly classified inputs. Since discovering the vulnerability of neural networks to adversarial examples [58], there have emerged numerous attacks in the literature, some of which have gained significant traction and are routinely used as benchmarks for evaluating both other attacks as well as detection mechanisms.

In our experiments, we also use such well-known attacks to evaluate the effectiveness of our approach against static adversaries. More specifically, we use the following six attacks:

- (1) Projected Gradient Descent (**PGD**) [36]
- (2) Fast Gradient Sign Method (**FGSM**) [23]
- (3) Basic Iterative Method (**BIM**) [31]
- (4) DeepFool (**DF**) [39]
- (5) Carlini-Wagner (**CW**) [13]
- (6) Jacobian Saliency Map Attack (**JSMA**) [45]

Each of these attacks specifies an upper bound on the amount of allowed distortion. This bound is typically defined in terms of norms, such as L_∞ , L_2 , and L_0 . For example, DF is an L_2 attack, meaning that the L_2 norm of original and adversarial inputs cannot be larger than a given bound. Regarding the above attacks, PGD,

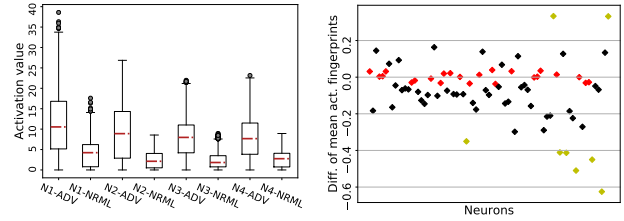


Figure 1: Differences in neuron activation values between normal and adversarial inputs.

FGSM, and BIM are L_∞ attacks, DF and CW L_2 , and JSMA L_0 . The L_2 attacks are found to be stronger than the others [13].

As we previously mentioned, these are white-box attacks of static adversaries. Attacks of adaptive adversaries are specifically tailored to the detection mechanism of the model under threat. Therefore, different detection mechanisms require different attacks, which means that there is no off-the-shelf adaptive adversary.

3 OUR APPROACH

Correctly classified (or normal) and adversarial inputs might look almost identical to the human eye. However, the *activation fingerprints*, that is, the neuron activation values, that these two kinds of inputs leave on a neural network are certainly different. This is because adversarial inputs cause the neural network to make a different prediction, and this difference is manifested through a change in the activation values of the neurons in the output network layer. For the activation values of these neurons to be different, there must also be changes in the activation values of neurons in previous layers.

As an example, we train a neural network on the MNIST [2] dataset for identifying handwritten-digit images. We then collect the activation values of four arbitrarily selected neurons for both normal and adversarial images, which are generated by the PGD attack. On the left of Fig. 1, we draw a box-plot of their activation values distinguishing between normal and adversarial images. As shown in the figure, there is a clear difference in the activation values of these neurons for the two kinds of images. In this paper, we present a Randomized Adversarial-Image Detection approach, which we call RAID, leveraging exactly this difference.

Fig. 2 gives an overview of RAID. In step 1, RAID provides a set of normal inputs to the neural network under threat, and for each input, records the activation values of every neuron. It also calculates the mean activation value of every neuron for all normal inputs. In step 2, RAID repeats this process for adversarial inputs that are generated by perturbing the normal inputs of the first step. In step 3, RAID selects a number of neurons to monitor based on the mean difference in activation values. In step 4, RAID trains a detection classifier based on the recorded activation values of the selected neurons.

To decide whether a new input is adversarial, RAID monitors the activation values of the selected neurons during prediction to obtain the fingerprint that is fed to the trained detection classifier.

3.1 Definitions

Let $N = \{n_1, n_2, \dots\}$ be the set of all neurons (excluding input and output layers) in a neural network \mathbb{NN} and $X = \{x_1, x_2, \dots\}$ an

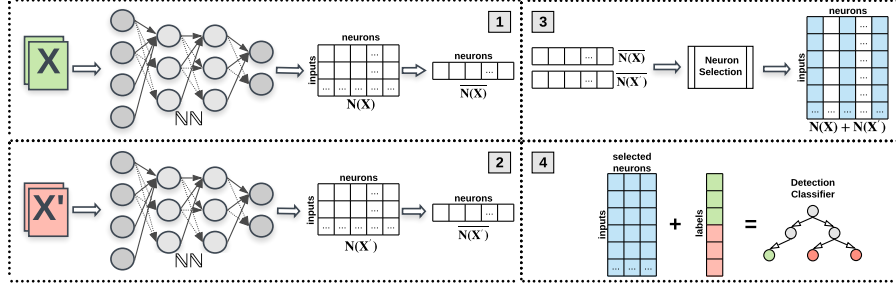


Figure 2: Overview of RAID.

arbitrary set of inputs. We denote the activation value of a neuron n_i for an input x_j as $n_i(x_j)$.

We call $n_i(X)$ the *activation-value block* of n_i with respect to inputs X , which essentially denotes a vector of activation values $n_i(x_j)$ for each input $x_j \in X$ (neuron n_i is fixed).

N stands for an ordered subset of all neurons N in the neural network. $N(x_j)$ denotes the *activation fingerprint* (AF) of input x_j on the neurons in subset N . The activation fingerprint is defined as a vector of activation values $n_i(x_j)$ for each neuron $n_i \in N$ (input x_j is fixed).

$N(X)$ yields a two-dimensional matrix, where each row corresponds to the activation fingerprint of an input $x_j \in X$ on neurons N and each column to the activation-value block of a neuron $n_i \in N$ with respect to inputs X .

We define a *mean activation fingerprint*, denoted $\overline{N(X)}$, as a vector that replaces each activation-value block in $N(X)$ by its mean activation value. Then, the *difference of mean activation fingerprints* for two sets of inputs X and Y is defined as $\overline{N(X)} - \overline{N(Y)}$, where the subtraction is performed element-wise.

3.2 RAID

RAID, is a simple, yet very effective, technique for detecting adversarial images. It is based on the key insight of leveraging differences in the activation fingerprints that normal and adversarial inputs leave on the NN under threat.

To make use of this insight, RAID starts by computing $N(X)$ and $N(X')$ for all neurons in NN , where X is a set of normal inputs, and X' the set of adversarial inputs generated by perturbing the inputs in X . In our experience, however, not all neurons behave differently for normal and adversarial inputs. For instance, it could be the case that, for a particular neuron n_i , the activation-value blocks $n_i(X)$ and $n_i(X')$ in $N(X)$ and $N(X')$, respectively, contain similar activation values.

On the right of Fig. 1, we plot the difference $\overline{N(M)} - \overline{N(M')}$ for all neurons in a simple neural network trained on the MNIST dataset. Here, M denotes the set of all images in MNIST and M' the adversarial images generated by DF. Each point in the figure corresponds to $\overline{n(M)} - \overline{n(M')}$, that is, the difference of mean activation-value blocks. Neurons with $|\overline{n(M)} - \overline{n(M')}| < 0.03$ appear in red, neurons with $|\overline{n(M)} - \overline{n(M')}| > 0.35$ in yellow, and the remaining neurons in black. We call red neurons *inessential* as their behavior does not change significantly for images in M and M' . Consequently, such neurons are not useful for detecting adversarial examples. On the

other hand, yellow neurons have a very clear difference in behavior and should be leveraged.

Our technique, therefore, filters out inessential neurons. More specifically, RAID computes and sorts the vector $|\overline{N(X)} - \overline{N(X')}|$. Then, based on a given percentage, which is a hyper-parameter of our technique called *filtering threshold*, RAID drops the percentage of this sorted vector with the lowest activation values.

RAID uses the activation values of the remaining *essential* neurons to train an adversarial-input detection classifier. In particular, our technique randomly selects a number of essential neurons to monitor, which is also a hyper-parameter of RAID. It then labels each AF of input $x \in X$ on the monitored neurons as normal, and each AF of $x' \in X'$ as adversarial. These AFs together with their labels are used to train our detection classifier. In Sect. 4, we show how the number of monitored neurons impacts the effectiveness of our technique. We also discuss why we *randomly* select the monitored neurons, instead of deterministically picking them.

The detection classifier takes the AF that a new input of the neural network leaves on the monitored neurons and decides whether the input is adversarial. Due to the relatively small number of monitored neurons, the input space of the detection classifier is not high dimensional, that is, the AFs do not have too many features. As a result, this allows us to choose a simple type of classifier without compromising the effectiveness of our approach. Instead of training a large detection neural network as in existing classifier-based work (e.g., [38]), our experiments demonstrate the competitive effectiveness of much simpler classifiers, such as decision trees, random forests, etc.

3.3 P-RAID: Pooled RAID

Existing classifier-based detection techniques [22, 24, 38] have been very successful in detecting adversarial examples. Despite their success, they have been criticized for being vulnerable to adaptive white-box attacks [11]. In particular, the criticism is that if a white-box attack can trick a neural network into making a wrong prediction, then it should also be able to bypass the detection classifier by adapting its adversarial attacks. We, therefore, extend our approach to be robust against adaptive white-box attacks. We refer to our extended technique as P-RAID, for Pooled-RAID.

The difference between RAID and P-RAID consists in training a *pool* of detection classifiers, instead of a single one. Each classifier in the pool is trained with the AFs left on an equal number of *randomly* selected essential neurons. These neurons are selected uniformly from the entire NN (after having filtered out the inessential neurons). This results in distinct classifiers, which however are

trained for the same goal. We pick an equal number of neurons for each classifier so that they are all similarly effective in detecting adversarial examples—recall that the number of monitored neurons impacts the effectiveness of the classifiers.

Now, for each new input of the neural network, P-RAID selects *uniformly at random* a detection classifier from the pool. The selected classifier determines if the input is adversarial. As we show in Sect. 4, extending our technique in this way does not impact its effectiveness. On the contrary, we argue that it improves its robustness against adaptive white-box attacks. Given that P-RAID picks the detection classifier *nondeterministically* for each input, an adaptive attacker would have to tailor its adversarial attacks to *all classifiers in the pool*. This is infeasible for three main reasons. First, the size of the pool can be arbitrarily large. Second, an attack that is optimized against one classifier might be impossible to also optimize against another since they are trained on different sets of neurons. Third, the pool of classifiers could contain different classifier types (e.g., k-nearest neighbors, random forests, etc.), which makes it even more difficult to tailor an attack to all classifiers.

4 EXPERIMENTAL EVALUATION

In this section, we address the following research questions using established evaluation guidelines for adversarial robustness [9, 11]:

- RQ1:** How effective is our approach in detecting adversarial images?
- RQ2:** Does our approach generalize within and across attack norms?
- RQ3:** How does our approach compare with state-of-the-art detection techniques?
- RQ4:** How does the selection of monitored neurons impact the effectiveness of our approach?
- RQ5:** How do multiple detection classifiers impact the effectiveness of our approach?
- RQ6:** How effective are different detection classifier types?

4.1 Implementation

We implemented (P-)RAID in Python using the popular machine-learning framework Keras [1] (v2.3.1) with the Tensorflow [3] (v1.15.0) back-end for analyzing neural networks. We also employ the scikit-learn library [47] for training detection classifiers. Last, we use IBM’s Adversarial Robustness Toolbox (ART) [41] for generating adversarial examples. Our implementation is open source.

4.2 Setup

We set up our experiments as follows.

Datasets and network models. We evaluate our technique on neural-network models trained on two popular datasets, namely MNIST [2] and CIFAR-10 [30]. MNIST is a dataset for recognizing handwritten-digit images, whereas the CIFAR-10 dataset focuses on recognizing objects and classifying them into ten categories. It is common to evaluate the effectiveness of adversarial-image detection techniques on these two datasets (e.g., [29, 60]). For MNIST, we trained a 5-layer convolutional neural network (ConvNet), with 320

neurons and 99.31% accuracy (when using 60,000 images for training and 10,000 for testing). For CIFAR-10, we trained a 12-layer ConvNet, with 2,208 neurons and 82.27% accuracy (when using 50,000 images for training and 10,000 for testing). These specific network models have also been used to evaluate a recent related technique [29].

Adversarial images. We generate adversarial images using six well-known attacks (see Sect. 2.2). The hyper-parameter configuration of each attack is given below:

- **PGD:** This is an iterative L_∞ -norm attack. We set the maximum number of iterations to 100 and the maximum distortion to 0.3 in terms of the L_∞ norm.
- **FGSM:** This is a one step L_∞ -norm attack. We set the maximum distortion to 0.3 in terms of the L_∞ norm.
- **BIM:** This attack is the iterative version of the FGSM attack. The maximum number of iterations is set to 100 and the maximum distortion to 0.3 in terms of the L_∞ norm.
- **DF:** This is an iterative L_2 -norm attack. We set the maximum number of iterations to 100.
- **CW:** Although there is an L_∞ -norm version of this attack, we employ its stronger L_2 -norm version [13]. We use the default settings of the ART library [41].
- **JSMA:** This is an L_0 -norm attack. We set parameter *gamma* bounding the fraction of perturbed features to 1.0.

We use each of these attacks to generate adversarial images in the following way. For each dataset, we split the test set, that is, the 10,000 images, into its halves. From each set of 5,000 original images, we remove any misclassified images and label the rest as normal. Next, we use each of the above attacks to generate 5,000 adversarial images for each set of normal images. We discard any generated images that are correctly classified and label the rest as adversarial. We then use one set of normal images together with its corresponding adversarial images to train a random-forest classifier based on the activation values of the monitored neurons. The remaining normal and adversarial images are used to test the ability of the classifier to detect adversarial images.

Existing detection techniques. In our experiments, we compare our approach with three state-of-the-art adversarial-image detection techniques from the literature [29, 60], two of which are classifier based and one is not.

Kim et al. [29] present two techniques based on the *surprise measure* of a given input to a neural network. They show that this surprise measure can be used to detect adversarial inputs, under the assumption that such inputs are more surprising than normal ones. The first technique presented in their paper, namely Likelihood-based Surprise Adequacy (LSA), is an extension of previous work [19]. In LSA, they estimate the probability density function of each neuron’s activation values, which is then used to measure how surprising an incoming input is. The second technique, namely Distance-based Surprise Adequacy (DSA), is a novel method based on the activation values of a set of neurons (i.e., a layer of neurons). In DSA, the surprise of an input x is measured by the distances between the activation-value vectors of the selected neurons from the closest input y in the same class and between y and the closest input z in a different class. Both LSA and DSA train

a classifier based on surprise values to distinguish adversarial and normal examples.

The third technique, mMutant [60], is based on the observation that, compared to a normal example, it is easier to change the class of an adversarial example via small mutations to the neural network. They first define the *label change rate* (LCR) of an input on slightly mutated versions of the original neural network. The LCR is found by dividing the number of predictions on mutated models deviating from the original prediction over the number of mutated models. The fundamental assumption behind mMutant is that the LCR of adversarial inputs is higher than the LCR of normal ones. We investigated the validity of this assumption, and our experiments suggest that it does not necessarily hold in general. Their paper provides a detection algorithm based on this assumption that tries to identify an LCR threshold for distinguishing between normal and adversarial inputs. However, this algorithm yields worse results [60] when compared to the AUC score achieved by the LCRs directly. For this reason, we do not consider it here.

For selecting hyper-parameters for the above techniques, we pick the configuration that achieves the best results. For LSA and DSA, we pick the best layers as proposed in the original paper since we use the same neural networks in our evaluation. For the attacks that are not included in the original paper, we still try to pick the layer that is the most effective. Note that, by re-optimizing hyper-parameters for each experiment, we give these two techniques a significant advantage over others (incl. RAID). The authors of mMutant describe four mutation operators for neural networks. We limit our comparison to Neuron Activation Inverse (NAI), which the authors show to be most effective.

Machine specifications. We conducted all our experiments on a 32-core Intel® Xeon® Gold 6134M CPU @ 3.20GH machine with 768GB of memory, running Debian v10.

4.3 Metrics

We evaluate the effectiveness of our approach using the following metrics.

Detection accuracy. The accuracy of a detection technique is a standard metric. For a set containing both normal and adversarial images, accuracy is the percentage of all images that are correctly detected as normal or adversarial. Higher accuracy suggests a better detection technique.

True-positive rate. We refer to the adversarial images that are correctly identified by our technique as *true positives* (TP), and to those that are incorrectly identified as *false negatives* (FN). The true-positive rate (TPR) is defined as $\frac{TP}{TP+FN}$ and denotes the ratio of correctly detected adversarial images over all adversarial images. A higher true-positive rate is better.

False-positive rate. We refer to the normal images that are correctly identified by our technique as *true negatives* (TN), and to those that are incorrectly identified as *false positives* (FP). The false-positive rate (FPR) is defined as $\frac{FP}{FP+TN}$ and denotes the ratio of normal images that are detected as adversarial over all normal images. A lower false-positive rate is better.

Area under curve of receiver operator characteristic. The receiver operator characteristic (ROC) curve plots the TPR against the FPR for all classification thresholds, which define the classification boundary between classes. Assuming that a detection classifier is expected to rank adversarial images higher than normal ones, the area under the ROC curve (AUC) denotes the probability that a randomly chosen adversarial image is ranked higher than a randomly chosen normal image. An AUC score that is closer to 1 is better.

4.4 Results

We now present our experimental results for each of the above research questions.

Unless stated otherwise, we configured our implementation to use exactly one classifier (not a pool), which is a random forest with 32 decision trees (or estimators). After filtering out 50% of the neurons in the networks for MNIST and CIFAR-10, the random forest is trained with the activation values of 64 randomly selected neurons.

We repeated all of our experiments 8 times, each time using a different random seed for the classifier and a different randomly selected set of neurons. Unless we explicitly state otherwise, the rest of this section reports mean results and their standard deviation.

RQ1: Adversarial-image detection. To measure the effectiveness of our approach in detecting adversarial images, we evaluate it against several well-known attacks. Tabs. 1 and 2 show the results for the MNIST and CIFAR-10 datasets, respectively.

The first column of the tables indicates the used attack. For instance, to obtain the results of the PGD row, we trained and tested our classifier using two different sets, each containing ~5,000 normal images as well as ~5,000 adversarial ones, which were generated by the PGD attack. Note that the number of images is approximate due to filtering, which is described in detail in Sect. 4.2. For L_2 , we trained and tested using ~5,000 normal images, ~5,000 adversarial images generated by DF, and ~5,000 adversarial images generated by CW. For L_∞ , we used PGD, FGSM, and BIM to generate adversarial images, and for L_* , all six attacks. Note that an L_0 row corresponds to the JSMA one as JSMA is the only L_0 attack used in our experiments. The remaining columns of the tables show the detection accuracy, the true- and false-positive rates, the area under the ROC curve, the number of true and false positives as well as the number of true and false negatives.

As shown in Tabs. 1 and 2, RAID is most effective in detecting L_∞ attacks, with accuracy, TPR, and AUC at 1.00 and FPR at 0.00, which constitute the theoretical best. RAID is least effective for L_2 attacks; this is to be expected since these are more powerful [11]. Naturally, the effectiveness for L_* lies in-between.

Tab. 3 shows the AUC score achieved by RAID when trained with normal and adversarial images generated by all attacks (L_*) and tested on normal and adversarial images generated by the attacks shown in the columns of the table. For example, when training RAID with all attacks, it achieves an AUC score of 1.0 when tested only on FGSM attacks. Again, our approach is most effective in detecting L_∞ attacks and slightly less effective for others.

Since RAID detects an adversarial image based on the prediction of a classifier, its running time for a single input is in the order of milliseconds. Training the classifier(s) used by (P-)RAID takes

Table 1: Effectiveness of RAID in detecting adversarial images generated by six attacks for MNIST.

	Accuracy	TPR	FPR	AUC	TP	FP	TN	FN
L_*	0.96 ± 0.00	0.99 ± 0.00	0.16 ± 0.02	0.99 ± 0.00	$23\,482.62 \pm 39.76$	813.50 ± 71.44	4089.50 ± 71.44	220.38 ± 39.76
L_∞	1.00 ± 0.00	1.00 ± 0.00	0.00 ± 0.00	1.00 ± 0.00	$14\,526.75 \pm 2.11$	9.38 ± 8.75	4893.62 ± 8.75	2.25 ± 2.11
L_2	0.94 ± 0.00	0.96 ± 0.01	0.09 ± 0.01	0.98 ± 0.00	8784.75 ± 44.74	423.50 ± 21.51	4479.50 ± 21.51	369.25 ± 44.74
PGD	1.00 ± 0.00	1.00 ± 0.00	0.00 ± 0.00	1.00 ± 0.00	4969.62 ± 0.86	5.75 ± 6.56	4897.25 ± 6.56	1.38 ± 0.86
FGSM	1.00 ± 0.00	1.00 ± 0.00	0.00 ± 0.00	1.00 ± 0.00	4617.00 ± 3.12	1.00 ± 1.12	4902.00 ± 1.12	2.00 ± 3.12
BIM	1.00 ± 0.00	1.00 ± 0.00	0.00 ± 0.00	1.00 ± 0.00	4936.38 ± 3.00	2.88 ± 4.73	4900.12 ± 4.73	2.62 ± 3.00
DF	0.94 ± 0.00	0.88 ± 0.01	0.01 ± 0.00	0.99 ± 0.00	3709.25 ± 34.23	68.25 ± 25.55	4834.75 ± 25.55	511.75 ± 34.23
CW	0.94 ± 0.01	0.93 ± 0.03	0.05 ± 0.01	0.98 ± 0.01	4633.50 ± 59.42	284.62 ± 13.90	4618.37 ± 13.90	299.50 ± 59.42
JSMA	0.95 ± 0.00	0.95 ± 0.01	0.06 ± 0.00	0.99 ± 0.00	4690.25 ± 9.87	285.38 ± 22.53	4617.62 ± 22.53	220.75 ± 9.87

Table 2: Effectiveness of RAID in detecting adversarial images generated by six attacks for CIFAR-10.

	Accuracy	TPR	FPR	AUC	TP	FP	TN	FN
L_*	0.95 ± 0.00	0.99 ± 0.00	0.34 ± 0.02	0.96 ± 0.00	$26\,346.56 \pm 8.67$	1230.78 ± 34.95	2360.22 ± 34.95	296.44 ± 8.67
L_∞	1.00 ± 0.00	1.00 ± 0.00	0.00 ± 0.00	1.00 ± 0.00	$14\,526.75 \pm 2.11$	9.38 ± 8.75	4893.62 ± 8.75	2.25 ± 2.11
L_2	0.88 ± 0.00	0.96 ± 0.00	0.30 ± 0.01	0.90 ± 0.00	7744.25 ± 9.27	1089.62 ± 30.60	2504.38 ± 30.60	358.75 ± 9.27
PGD	1.00 ± 0.00	1.00 ± 0.00	0.00 ± 0.00	1.00 ± 0.00	4781.25 ± 0.83	0.50 ± 0.71	3587.50 ± 0.71	0.75 ± 0.83
FGSM	1.00 ± 0.00	1.00 ± 0.00	0.00 ± 0.00	1.00 ± 0.00	4289.00 ± 0.00	0.00 ± 0.00	3588.00 ± 0.00	0.00 ± 0.00
BIM	1.00 ± 0.00	1.00 ± 0.00	0.00 ± 0.00	1.00 ± 0.00	3588.00 ± 0.00	0.00 ± 0.00	0.00 ± 0.00	4631.00 ± 0.00
DF	0.83 ± 0.00	0.87 ± 0.00	0.20 ± 0.00	0.91 ± 0.00	3470.00 ± 17.36	719.88 ± 19.76	2874.12 ± 19.76	535.00 ± 17.36
CW	0.85 ± 0.00	0.93 ± 0.01	0.24 ± 0.01	0.91 ± 0.01	3816.25 ± 14.62	842.50 ± 32.76	2745.50 ± 32.76	281.75 ± 14.62
JSMA	0.90 ± 0.00	0.93 ± 0.01	0.13 ± 0.01	0.96 ± 0.00	4470.75 ± 31.95	481.38 ± 25.27	3106.62 ± 25.27	364.25 ± 31.95

longer, but this process is performed once and offline. Training time depends on three factors: (1) number of training inputs, (2) number of features in each input, and (3) internal complexity of the classifier(s) (e.g., number of estimators in a random forest). For RAID’s best configuration described at the beginning of this subsection, training a random forest with 10,000 images takes less than 30 seconds.

RQ2: Attack norms. We refer to L_0 , L_2 , L_∞ , and L_* as attack norms. This research question focuses on evaluating whether RAID’s detection generalizes within and across attack norms.

Within an attack norm, we train with (normal and) adversarial images generated by an attack of a particular norm (e.g., PGD for L_∞ , DF for L_2) and measure the AUC score achieved by RAID when testing with (normal and) adversarial images generated by a different attack of the same norm (e.g., FGSM for L_∞ , CW for L_2). The results for L_∞ are shown in Tab. 4, and for L_2 in Tab. 5. The first column of the tables refers to the attack with which we train, whereas the first row indicates the used dataset as well as the attack with which we test.

Table 3: AUC scores achieved by RAID when trained with all and tested on a subset of attacks.

	L_∞	L_2	PGD	FGSM	BIM	DF	CW	JSMA
MNIST	1.00	0.97	1.00	1.00	1.00	0.99	0.97	0.98
CIFAR-10	1.00	0.89	1.00	1.00	1.00	0.90	0.89	0.94

The results in Tab. 4 are impressive. RAID achieves the best possible AUC score with 0.00 standard deviation for all attacks within L_∞ . Therefore, our detection technique generalizes perfectly within this norm. As shown in Tab. 5 however, RAID does not generalize as well within the L_2 norm. The AUC scores in this table are slightly lower than those in Tabs. 1 and 2, where we trained with L_2 , DF, or CW and tested with the same. This also holds when comparing with the scores in Tab. 3, where we trained with all attacks and tested with L_2 , DF, or CW. These results indicate that, for the more powerful L_2 norm, our detection technique is more effective when trained with the attack it is expected to detect.

Across attack norms, we train with (normal and) adversarial images generated by all attacks of a particular norm (e.g., PGD, FGSM, and BIM of L_∞) and measure the AUC score achieved by RAID when testing with (normal and) adversarial images generated by all attacks of a different norm (e.g., DF and CW of L_2). The results are shown in Tab. 6. The first column of the table refers to

Table 4: AUC scores achieved by RAID when trained with a particular attack of the L_∞ norm (shown in the first column) and tested with another of the same norm (first row).

	MNIST			CIFAR-10		
	PGD	FGSM	BIM	PGD	FGSM	BIM
PGD	1.00	1.00	1.00	1.00	1.00	1.00
FGSM	1.00	1.00	1.00	1.00	1.00	1.00
BIM	1.00	1.00	1.00	1.00	1.00	1.00

Table 5: AUC scores achieved by RAID when trained with a particular attack of the L_2 norm (shown in the first column) and tested with another of the same norm (first row).

	MNIST		CIFAR-10	
	DF	CW	DF	CW
DF		0.88		0.86
CW	0.88		0.86	

the norm with which we train, whereas the first row indicates the used dataset as well as the norm with which we test.

As previously observed (Tab. 3), when training with L_* , our technique is most effective in detecting L_∞ attacks and only slightly less effective for other norms. When training with L_2 , RAID’s detection generalizes quite well to all other attack norms (L_* , L_∞ , and L_0). The same holds when training with L_0 , although this configuration is less effective for the CIFAR-10 dataset. These results suggest that training with stronger attacks generalizes to detecting weaker ones. On the other hand, when training with the weaker L_∞ attacks, the AUC scores for the detection of L_2 and L_0 attacks drop significantly.

RQ3: Comparison with state of the art. We now compare RAID with the three state-of-the-art detection techniques discussed in Sect. 4.2, namely DSA, LSA, and mMutant.

For this experiment, we measure the AUC score achieved by each technique when tested with each attack and attack norm. The results are shown in Fig. 3 for MNIST and Fig. 4 for CIFAR-10. For the techniques that require training, that is, for RAID, DSA, and LSA, we train with L_* . We chose this configuration because it is the most general, and thus, the most natural. In practice, a detection technique is not a-priori aware of the type or norm of future attacks; it is, therefore, safer to anticipate all of them.

To obtain the AUC scores in the figures, we test each technique using normal and adversarial images, which are generated by the attacks shown on the x-axes of the bar charts. In addition to the aforementioned attacks, we add two more for this experiment. First, we simulate an adaptive adversary against mMutant by introducing CW-0.95, which is exactly the same as CW except that the *confidence* parameter is set to 0.95. In other words, CW-0.95 generates adversarial images classified with a prediction confidence of at least 0.95 at the expense of adding more distortion. Note that we only add this attack for CIFAR-10 since CW cannot generate adversarial inputs with high confidence on MNIST. Second, we introduce CW-Noise denoting that our test set contains, in addition to the $\sim 5,000$ normal images, $\sim 5,000$ adversarial images generated by CW as well as $\sim 5,000$ normal images with Gaussian noise (mean=0, std=0.2) by following the guidelines presented in [9]. We apply the filtering described in Sect. 4.2 on the test sets of all techniques.

As shown in Fig. 3, the effectiveness of RAID, DSA, and LSA is comparable on the MNIST dataset. In the best case, RAID outperforms DSA by 0.05 for CW, and LSA by 0.03 for CW-0.95. In the worst case, LSA outperforms RAID by 0.02 for CW-Noise. The effectiveness of mMutant varies significantly. For example, it outperforms all other techniques for the powerful CW attacks, but is substantially worse for the simple PGD attacks. This is because mMutant is based on the assumption that adversarial examples are

Table 6: AUC scores of RAID when trained with a particular norm (first column) and tested with another (first row).

	MNIST				CIFAR-10			
	L_*	L_∞	L_2	L_0	L_*	L_∞	L_2	L_0
L_*		1.00	0.97	0.98		1.00	0.89	0.94
L_∞	0.84		0.67	0.68	0.77		0.54	0.52
L_2	0.96	0.96		0.95	0.92	0.95		0.91
L_0	0.92	0.90	0.91		0.81	0.73	0.85	

sensitive to mutations, that is, they are typically classified with a low prediction confidence. However, iterative attacks such as BIM and PGD generate adversarial images with very high prediction confidence (e.g., 0.99 almost all the time), which makes them more insensitive, and hence, harder to detect by mMutant. In this sense, the more distortion is added to the input, the lower the chance that mMutant detects it since higher distortion typically increases prediction confidence.

Fig. 4 shows the same comparison for CIFAR-10. Here, RAID consistently outperforms DSA and LSA, namely for L_* , L_∞ , L_2 , FGSM, BIM, DF, CW, CW-Noise, and JSMA. Their effectiveness is equal for PGD, and DSA outperforms RAID by 0.02 for CW-0.95. RAID outperforms mMutant for L_* , L_∞ , PGD, FGSM, BIM, CW-0.95, and CW-Noise, in the best case by 0.88 for PGD and in the worst case by 0.09 for FGSM. On the other hand, mMutant looks slightly more effective than RAID for L_2 (by 0.03), DF (by 0.01), CW (by 0.04), and JSMA (by 0.03). However, as shown with CW-0.95, increasing prediction confidence for these cases would reduce mMutant’s effectiveness.

In addition to (often significantly) outperforming state-of-the-art detection techniques, RAID is also the most consistent in terms of effectiveness across different types of attacks and norms. Tab. 7 shows the ranges of AUC scores achieved by RAID, DSA, LSA, and mMutant for the attacks in Figs. 3 and 4. As shown in the table, the ranges are more stable for RAID than for any other technique.

In terms of performance, RAID is also very efficient. At runtime, RAID requires (1) feeding the incoming input to the original neural network to collect its AF and (2) feeding the AF to the detection classifier; in total, this takes less than a second as described in RQ1. LSA, DSA, and mMutant demonstrate a similarly good runtime performance. mMutant requires feeding the input to a number of mutated neural networks (default is 500). Given that each neural-network query takes less than a millisecond, mMutant can make a decision under 1 second. Note that, although model mutation takes much more time (i.e., per mutation slightly more than 5 seconds for MNIST and slightly more than 15 seconds for CIFAR-10), it is performed offline and incurs no runtime overhead. Similarly to RAID, LSA and DSA involve feeding the input to the original network and then feeding the extracted data to the classifier; overall, these steps also take around 1 second.

RQ4: Selection of monitored neurons. To determine how the selection of monitored neurons impacts the effectiveness of our technique, we first measure the AUC scores achieved by RAID for different numbers of monitored neurons, namely 1, 4, 16, 64, and 256 (or all essential neurons if their total number is smaller than

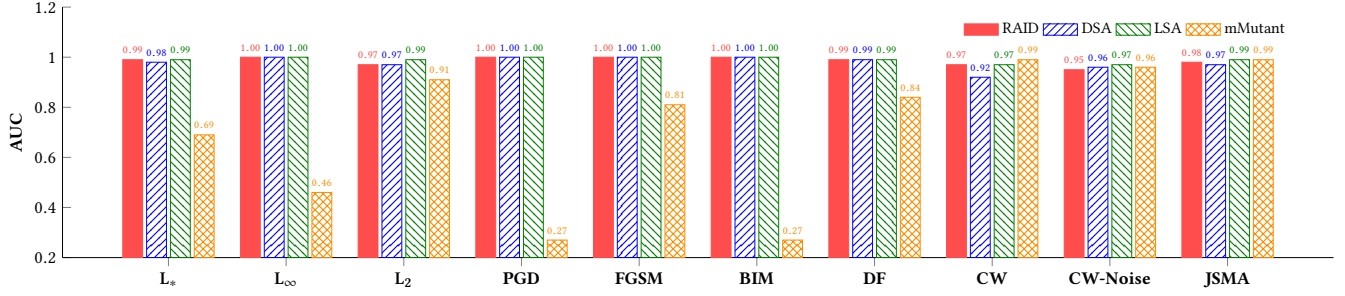


Figure 3: AUC scores of RAID, DSA, LSA, and mMutant on the MNIST dataset when tested on all attacks and norms.

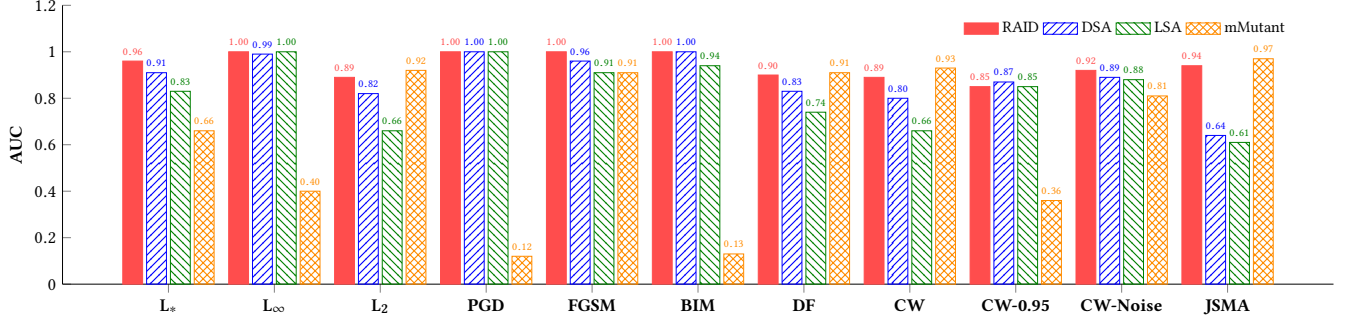


Figure 4: AUC scores of RAID, DSA, LSA, and mMutant on the CIFAR-10 dataset when tested on all attacks and norms.

256). For this experiment, we train and test RAID on each attack norm. The results are presented in Fig. 5, where the plot on the left is for MNIST and the plot on the right for CIFAR-10.

As shown in the figure, more neurons lead to better AUC scores, although the differences are insignificant when comparing 64 and 256 neurons. This is expected because the larger the number of monitored neurons, the higher are the chances of correctly detecting more normal and adversarial examples. In particular, the activation value of a neuron may fluctuate only for a specific set of normal and adversarial images, whereas the activation value of another neuron may fluctuate for a completely disjoint set. Therefore, when monitoring both of these neurons, our technique is likely to be more effective. In practice, with only a single neuron to monitor, RAID may be lucky with its selection as for L_∞ and CIFAR-10 in Fig. 5, but this is typically not the case as is also shown in the figure.

To further investigate the impact of monitored neurons on our technique, we also performed the same experiment when selecting the best neurons, that is, those with the largest difference of mean activation fingerprints (see Sect. 3.2), and when selecting the worst neurons. Note that the worst neurons are normally filtered out by our technique as inessential. The results are shown in Figs. 6 and 7. For this experiment, unlike for the one in Fig. 5, we do not perform 8 runs of RAID since the sets of best and worst neurons are chosen deterministically.

Table 7: Range of AUC scores achieved by RAID, DSA, LSA, and mMutant when tested on the attacks of Figs. 3 and 4.

	RAID	DSA	LSA	mMutant
MNIST	0.95–1.00	0.92–1.00	0.93–1.00	0.27–0.99
CIFAR-10	0.85–1.00	0.64–1.00	0.61–1.00	0.12–0.97

When comparing the AUC scores of Figs. 5 and 6, we observe that selecting the best neurons mostly benefits configurations with a small number of neurons. For 64 neurons, which is the configuration used throughout our experiments, RAID with the best neurons is better only for L_∞ and MNIST and only by 0.01, which justifies the value of our filtering threshold (50%). Interestingly, some AUC scores achieved by RAID with the best neurons are slightly worse than those with random neurons. This may happen when the activation values of the best neurons fluctuate for overlapping sets of images, whereas there are worse neurons that would help with the detection of other images.

The AUC scores achieved by RAID when selecting the worst neurons (Fig. 7) are significantly worse than those in Figs. 5 and 6, which justifies the existence of our filtering threshold. For CIFAR-10, all AUC scores are 0.5. This is because the neural network for the CIFAR-10 dataset has a much larger number of neurons in comparison to the network for MNIST (see Sect. 4.2). Consequently, there are also many more inessential neurons.

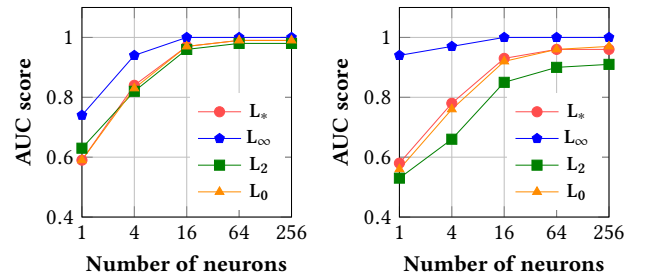


Figure 5: AUC scores of RAID for all attack norms versus the number of neurons (left: MNIST, right: CIFAR-10).

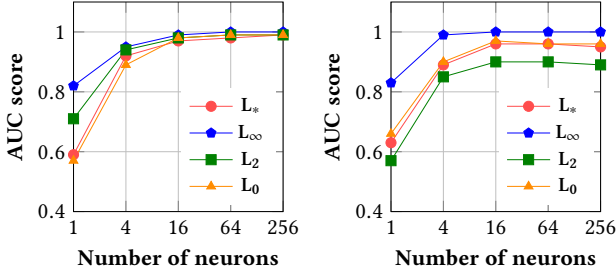


Figure 6: AUC scores of RAID for all norms when monitoring the best neurons (left: MNIST, right: CIFAR-10).

RQ5: Multiple classifiers. As explained in Sect. 3.3, P-RAID is the robust version of RAID against adaptive adversaries. In this research question, we investigate the effectiveness of a pool of classifiers versus a single classifier. In particular, we compare the AUC scores achieved by RAID and P-RAID, with a pool size of 32 random forests (each with 32 estimators). We trained both tools with the expected attacks (e.g., trained with FGSM and tested with FGSM). The results are presented in Tab. 8.

As shown in the table, the effectiveness of the tools is almost identical. We mark the three differences in bold; the achieved AUC scores differ by 0.01 across the two implementations. Consequently, using the P-RAID version of our approach has no negative impact on its success in detecting adversarial images. On the contrary, it offers the theoretical benefit of being more powerful against adaptive adversaries.

On the other hand, state-of-the-art tools mentioned in RQ3 do not claim robustness against adaptive adversaries. The original idea behind LSA is already shown to be bypassed [11]. For DSA, there is no specific mechanism against adaptive adversaries, and such classifier-based detectors are typically found to be weak against adaptive adversaries [11]. In our experiments, we show the weakness of mMutant by introducing CW-0.95.

RQ6: Different classifier types. We now study the impact of different classifier types and their parameters on the effectiveness of our approach. In particular, we use the following classifier types:

DT: Decision tree [49]

RF: Random forest with 32, 64, and 128 estimators [7]

AB: AdaBoost with 32, 64, and 128 estimators [51]

KNN: k -nearest neighbors with 3 and 5 neighbors [5, 43]

We selected these classifiers because they are simple when compared to huge detection networks [38], on the other hand, they

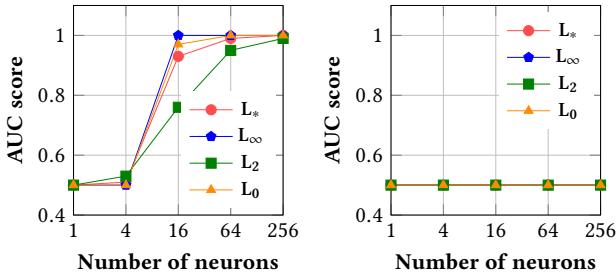


Figure 7: AUC scores of RAID for all norms when monitoring the worst neurons (left: MNIST, right: CIFAR-10).

Table 8: AUC scores achieved by RAID and P-RAID when trained and tested on the same attacks.

	MNIST		CIFAR-10	
	RAID	P-RAID	RAID	P-RAID
L_*	0.99 ± 0.00	0.99 ± 0.01	0.96 ± 0.00	0.96 ± 0.01
L_{∞}	1.00 ± 0.00	1.00 ± 0.00	1.00 ± 0.00	1.00 ± 0.00
L_2	0.98 ± 0.00	0.98 ± 0.01	0.90 ± 0.00	0.90 ± 0.02
PGD	1.00 ± 0.00	1.00 ± 0.00	1.00 ± 0.00	1.00 ± 0.00
FGSM	1.00 ± 0.00	1.00 ± 0.00	1.00 ± 0.00	1.00 ± 0.00
BIM	1.00 ± 0.00	1.00 ± 0.00	1.00 ± 0.00	1.00 ± 0.00
DF	0.99 ± 0.00	0.98 ± 0.00	0.91 ± 0.00	0.91 ± 0.02
CW	0.98 ± 0.01	0.98 ± 0.01	0.91 ± 0.01	0.90 ± 0.02
JSMA	0.99 ± 0.00	0.99 ± 0.01	0.96 ± 0.00	0.96 ± 0.01

are known to be effective in many tasks. Note that RF and AB are referred to as ensemble methods because they consist of multiple classifiers, in this case decision trees.

For this experiment, we train one classifier of each type (not a pool) with the expected attack norms. We then measure the AUC scores achieved by RAID when using each of these classifiers. The results are presented in Figs. 8 and 9 for MNIST and CIFAR-10, respectively. As shown in the bar charts, the ensemble methods RF and AB are more effective than DT and KNN on the two datasets. KNN is slightly better than AB for MNIST, but noticeably worse for CIFAR-10. These results suggest that ensembles of simple classifiers, such as decision trees, are sufficient for our approach to be very effective in practice.

Out of the two ensemble methods, RF is more effective than AB. The number of RF estimators does not have a significant impact on the AUC scores. Specifically, when using 64 estimators, the AUC scores can increase by up to 0.01 in comparison to 32 estimators (for L_2 attacks in both datasets, and for L_0 in CIFAR-10). There is also no difference between using 64 and 128 estimators. Recall, however, that the number of estimators affects the training time, and therefore, RF32 can be trained more efficiently.

4.5 Threats to Validity

We identify the following threats to the validity of our experiments.

External validity. External validity ensures that the results of an experimental evaluation generalize [54]. Our results may not generalize to other datasets or network models [54]. However, we use two of the most popular datasets for evaluating state-of-the-art adversarial-image detection techniques (e.g., [29, 60]) and borrow the models from one of these techniques [29]. The results may also not generalize to other attacks although we generate adversarial images using six well-known attacks across three attack norms.

In our evaluation, we compare RAID with three adversarial-image detection techniques, but our results may not generalize to others [54]. To alleviate this threat, we selected the most recent detection techniques published at top venues. Moreover, our implementation is open source so that others can reproduce our results and perform more extensive comparisons.

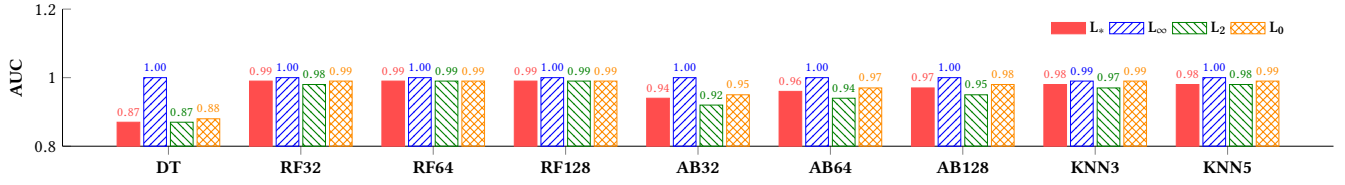


Figure 8: AUC scores achieved by RAID on the MNIST dataset when using different classifier types.

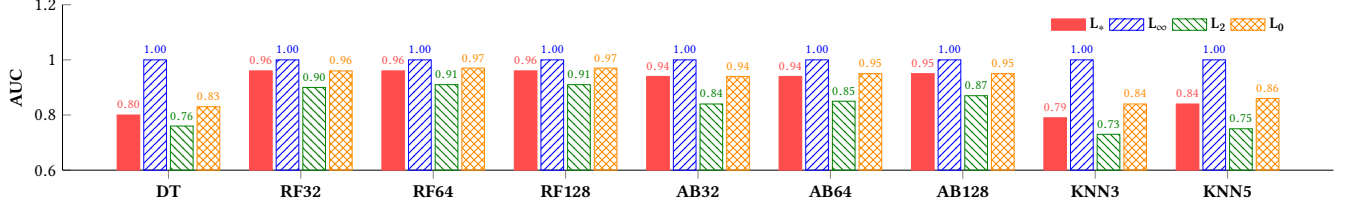


Figure 9: AUC scores achieved by RAID on the CIFAR-10 dataset when using different classifier types.

Internal validity. The internal validity [54] of randomized approaches may be compromised by a potentially biased selection of random seeds. We avoid this pitfall by performing all of our experiments 8 times, each time using a different random seed for the classifier and a different randomly selected set of neurons. We report mean results and their standard deviation.

5 RELATED WORK

Adversarial robustness. The area of adversarial machine learning has been very active since the discovery of adversarial examples for neural networks [58]. On one side, more effective adversarial attacks are being developed. On the other side, researchers develop new techniques to obtain *robust* neural networks. Here, we consider two types of robustness techniques: (1) those that *detect* adversarial examples, and (2) those that aim to build a network for which it is difficult to generate adversarial examples, namely *defenses*. According to this classification, RAID falls into the first category.

Adversarial-input detection. Despite these efforts to ensure robustness of neural networks, new attacks often evade existing defense or detection techniques. On the detection side, Grosse et al., Gong et al., and Metzen et al. [22, 24, 38] train a secondary classifier for detecting adversarial examples; in this aspect, these techniques are similar to ours. From these three, the approach presented by Metzen et al. [38] is the closest to our work. However, unlike their technique, we propose a much simpler methodology and an extension (i.e., in P-RAID) to handle adaptive adversaries. Hendrycks and Gimpel, Bhagoji et al., and Li and Li [6, 26, 32] propose methods based on Principal Component Analysis (PCA). Feinman et al. [19] introduce two techniques, called kernel-density estimation and Bayesian neural-network uncertainty. Carlini and Wagner [11], however, find all of the aforementioned techniques ineffective for providing a thorough detection mechanism.

While there are other works that claim to be effective in detecting adversarial inputs, they have already been surpassed or bypassed by later work. For example, work on statistical detection [50] can be bypassed [27]. Similarly, feature squeezing [62] can be defeated [53], and both methods by Zantedeschi et al. [63] and MagNet [37] are shown not to be robust [12, 33].

Even more recent detection techniques include work that specializes on adaptive adversaries [28], focuses on black-box attacks [14], and makes use of the SHAP explainability technique [20]. Lastly, two detection techniques [29, 60] have recently been proposed by the software-engineering community. We provide a detailed description of these in the previous section, where we compare them with RAID.

Defenses against adversarial inputs. On the defense side, adversarial retraining was found to be effective [36]. Despite this, many defenses [40, 46] are circumvented by other work [4, 10, 25]. Generally, one should follow recent guidelines for properly evaluating the robustness of a neural network [9].

Neural-network testing. The increasing popularity of deep-learning systems and their vulnerability to adversarial examples also motivated research into testing techniques for neural networks. Existing research in the area adapts testing methodologies from traditional software engineering. DeepXplore [48] is the first to introduce a specialized coverage criterion (i.e., neuron coverage) for neural networks. Subsequently, new such coverage criteria have been proposed. For example, DeepGauge [34] refines neuron coverage, DeepCover [55] adapts MC/DC from traditional software testing, and DeepCT [35] investigates combinatorial testing. However, more recent work argues that there is limited correlation between coverage and robustness of neural networks [16].

Eniser et al. [17] make use of fault-localization metrics for finding neurons that can be exploited to fool networks. Sun et al. [56] adapt concolic testing [8, 21, 52] for generating test inputs to neural networks. Other approaches make use of coverage-guided fuzzing for input generation [15, 42, 61]. DeepTest [59] and DeepRoad [64] focus on generating test inputs for deep-learning-based autonomous driving systems. Unlike the above testing techniques, RAID proposes an *online* detection technique for adversarial examples.

6 CONCLUSION

In this work, we propose a novel mechanism, namely RAID, for detecting adversarial examples in neural networks. In addition to this, we introduce P-RAID, which is designed to be robust even against adaptive adversaries. We extensively evaluate our technique and

show its effectiveness, for instance by achieving a 90% AUC score against the strongest attacks (i.e., CW, DF) and perfect detection against weaker adversaries (i.e., PGD, BIM, FGSM). The comparison with three state-of-the-art detection techniques shows that RAID is both more stable and more effective. In the future, we plan to test our tool on other threat models, larger neural networks, and different tasks, such as natural language processing.

REFERENCES

- [1] [n.d.]. Keras: The Python Deep Learning Library. <https://keras.io>.
- [2] [n.d.]. The MNIST Database of Handwritten Digits. <http://yann.lecun.com/exdb/mnist>.
- [3] [n.d.]. TensorFlow: Large-Scale Machine Learning on Heterogeneous Systems. <https://www.tensorflow.org>.
- [4] Anish Athalye, Nicholas Carlini, and David A. Wagner. 2018. Obfuscated Gradients Give a False Sense of Security: Circumventing Defenses to Adversarial Examples. In *ICML (PMLR)*, Vol. 80. PMLR, 274–283.
- [5] Jon Louis Bentley. 1975. Multidimensional Binary Search Trees Used for Associative Searching. *CACM* 18 (1975), 509–517. Issue 9.
- [6] Arjun Nitin Bhagoji, Daniel Cullina, and Prateek Mittal. 2017. Dimensionality Reduction as a Defense Against Evasion Attacks on Machine Learning Classifiers. *CoRR* abs/1704.02654 (2017).
- [7] Leo Breiman. 2001. Random Forests. *Machine Learning* 45 (2001), 5–32. Issue 1.
- [8] Cristian Cadar and Dawson R. Engler. 2005. Execution Generated Test Cases: How to Make Systems Code Crash Itself. In *SPIN (LNCS)*, Vol. 3639. Springer, 2–23.
- [9] Nicholas Carlini, Anish Athalye, Nicolas Papernot, Wieland Brendel, Jonas Rauber, Dimitris Tsipras, Ian J. Goodfellow, Aleksander Madry, and Alexey Kurakin. 2019. On Evaluating Adversarial Robustness. *CoRR* abs/1902.06705 (2019).
- [10] Nicholas Carlini and David A. Wagner. 2016. Defensive Distillation is Not Robust to Adversarial Examples. *CoRR* abs/1607.04311 (2016).
- [11] Nicholas Carlini and David A. Wagner. 2017. Adversarial Examples Are Not Easily Detected: Bypassing Ten Detection Methods. In *AISeC@CCS*. ACM, 3–14.
- [12] Nicholas Carlini and David A. Wagner. 2017. MagNet and “Efficient Defenses Against Adversarial Attacks” Are Not Robust to Adversarial Examples. *CoRR* abs/1711.08478 (2017).
- [13] Nicholas Carlini and David A. Wagner. 2017. Towards Evaluating the Robustness of Neural Networks. In *S&P*. IEEE Computer Society, 39–57.
- [14] Steven Chen, Nicholas Carlini, and David A. Wagner. 2019. Stateful Detection of Black-Box Adversarial Attacks. *CoRR* abs/1907.05587 (2019).
- [15] Samet Demir, Hasan Ferit Eniser, and Alper Sen. 2019. DeepSmartFuzzer: Reward Guided Test Generation For Deep Learning. *CoRR* abs/1911.10621 (2019).
- [16] Yizhen Dong, Peixin Zhang, Jingyi Wang, Shuang Liu, Jun Sun, Jianye Hao, Xinyu Wang, Li Wang, Jin Song Dong, and Dai Ting. 2019. There is Limited Correlation between Coverage and Robustness for Deep Neural Networks. *CoRR* abs/1911.05904 (2019).
- [17] Hasan Ferit Eniser, Simos Gerasimou, and Alper Sen. 2019. DeepFault: Fault Localization for Deep Neural Networks. In *FASE (LNCS)*, Vol. 11424. Springer, 171–191.
- [18] Kevin Eykholt, Ivan Evtimov, Earlene Fernandes, Bo Li, Amir Rahmati, Chaowei Xiao, Atul Prakash, Tadayoshi Kohno, and Dawn Song. 2018. Robust Physical-World Attacks on Deep Learning Visual Classification. In *CVPR*. IEEE Computer Society, 1625–1634.
- [19] Reuben Feinman, Ryan R. Curtin, Saurabh Shintre, and Andrew B. Gardner. 2017. Detecting Adversarial Samples from Artifacts. *CoRR* abs/1703.00410 (2017).
- [20] Gil Fidel, Ron Bitton, and Asaf Shabtai. 2019. When Explainability Meets Adversarial Learning: Detecting Adversarial Examples Using SHAP Signatures. *CoRR* abs/1909.03418 (2019).
- [21] Patrice Godefroid, Nils Klarlund, and Koushik Sen. 2005. DART: Directed Automated Random Testing. In *PLDI*. ACM, 213–223.
- [22] Zhitao Gong, Wenlu Wang, and Wei-Shinn Ku. 2017. Adversarial and Clean Data Are Not Twins. *CoRR* abs/1704.04960 (2017).
- [23] Ian J. Goodfellow, Jonathon Shlens, and Christian Szegedy. 2015. Explaining and Harnessing Adversarial Examples. In *ICLR*.
- [24] Kathrin Grosse, Praveen Manoharan, Nicolas Papernot, Michael Backes, and Patrick D. McDaniel. 2017. On the (Statistical) Detection of Adversarial Examples. *CoRR* abs/1702.06280 (2017).
- [25] Warren He, James Wei, Xinyun Chen, Nicholas Carlini, and Dawn Song. 2017. Adversarial Example Defense: Ensembles of Weak Defenses Are Not Strong. In *WOOT. USENIX*.
- [26] Dan Hendrycks and Kevin Gimpel. 2017. Early Methods for Detecting Adversarial Images. In *ICLR (Workshop)*. OpenReview.net.
- [27] Hossein Hosseini, Sreeram Kannan, and Radha Poovendran. 2019. Are Odds Really Odd? Bypassing Statistical Detection of Adversarial Examples. *CoRR* abs/1907.12138 (2019).
- [28] Shengyuan Hu, Tao Yu, Chuan Guo, Wei-Lun Chao, and Kilian Q. Weinberger. 2019. A New Defense Against Adversarial Images: Turning a Weakness into a Strength. In *NeurIPS*. 1633–1644.
- [29] Jinhan Kim, Robert Feldt, and Shin Yoo. 2019. Guiding Deep Learning System Testing Using Surprise Adequacy. In *ICSE*. IEEE Computer Society/ACM, 1039–1049.
- [30] Alex Krizhevsky. 2009. *Learning Multiple Layers of Features from Tiny Images*. Technical Report. University of Toronto.

- [31] Alexey Kurakin, Ian J. Goodfellow, and Samy Bengio. 2017. Adversarial Examples in the Physical World. In *ICLR*. OpenReview.net.
- [32] Xin Li and Fuxin Li. 2017. Adversarial Examples Detection in Deep Networks with Convolutional Filter Statistics. In *ICCV*. IEEE Computer Society, 5775–5783.
- [33] Pei-Hsuan Lu, Pin-Yu Chen, Kang-Cheng Chen, and Chia-Mu Yu. 2018. On the Limitation of MagNet Defense Against L1-Based Adversarial Examples. In *DSN Workshops*. IEEE Computer Society, 200–214.
- [34] Lei Ma, Felix Juefei-Xu, Fuyuan Zhang, Jiyuan Sun, Minhui Xue, Bo Li, Chunyang Chen, Ting Su, Li Li, Yang Liu, Jianjun Zhao, and Yadong Wang. 2018. DeepGauge: Multi-Granularity Testing Criteria for Deep Learning Systems. In *ASE*. ACM, 120–131.
- [35] Lei Ma, Fuyuan Zhang, Minhui Xue, Bo Li, Yang Liu, Jianjun Zhao, and Yadong Wang. 2018. Combinatorial Testing for Deep Learning Systems. *CoRR* abs/1806.07723 (2018).
- [36] Aleksander Madry, Aleksandar Makelov, Ludwig Schmidt, Dimitris Tsipras, and Adrian Vladu. 2018. Towards Deep Learning Models Resistant to Adversarial Attacks. In *ICLR*. OpenReview.net.
- [37] Dongyu Meng and Hao Chen. 2017. MagNet: A Two-Pronged Defense Against Adversarial Examples. In *CCS*. ACM, 135fi?–147.
- [38] Jan Hendrik Metzen, Tim Genewein, Volker Fischer, and Bastian Bischoff. 2017. On Detecting Adversarial Perturbations. *CoRR* abs/1702.04267 (2017).
- [39] Seyed-Mohsen Moosavi-Dezfooli, Alhussein Fawzi, and Pascal Frossard. 2016. DeepFool: A Simple and Accurate Method to Fool Deep Neural Networks. In *CVPR*. IEEE Computer Society, 2574–2582.
- [40] Aran Nayebi and Surya Ganguli. 2017. Biologically Inspired Protection of Deep Networks from Adversarial Attacks. *CoRR* abs/1703.09202 (2017).
- [41] Maria-Irina Nicolae, Mathieu Sinn, Tran Ngoc Minh, Amrith Rawat, Martin Wistuba, Valentina Zantedeschi, Ian M. Molloy, and Benjamin Edwards. 2018. Adversarial Robustness Toolbox v0.2.2. *CoRR* abs/1807.01069 (2018).
- [42] Augustus Odena, Catherine Olsson, David Andersen, and Ian J. Goodfellow. 2019. TensorFuzz: Debugging Neural Networks with Coverage-Guided Fuzzing. In *ICML (PMLR)*, Vol. 97. PMLR, 4901–4911.
- [43] Stephen M. Omohundro. 1989. *Five Balltree Construction Algorithms*. Technical Report. ICSI.
- [44] Nicolas Papernot, Patrick D. McDaniel, Ian J. Goodfellow, Somesh Jha, Z. Berkay Celik, and Ananthram Swami. 2017. Practical Black-Box Attacks Against Machine Learning. In *AsiaCCS*. ACM, 506–519.
- [45] Nicolas Papernot, Patrick D. McDaniel, Somesh Jha, Matt Fredrikson, Z. Berkay Celik, and Ananthram Swami. 2016. The Limitations of Deep Learning in Adversarial Settings. In *EuroS&P*. IEEE Computer Society, 372–387.
- [46] Nicolas Papernot, Patrick D. McDaniel, Xi Wu, Somesh Jha, and Ananthram Swami. 2016. Distillation as a Defense to Adversarial Perturbations Against Deep Neural Networks. In *S&P*. IEEE Computer Society, 582–597.
- [47] Fabian Pedregosa, Gaël Varoquaux, Alexandre Gramfort, Vincent Michel, Bertrand Thirion, Olivier Grisel, Mathieu Blondel, Peter Prettenhofer, Ron Weiss, Vincent Dubourg, Jake VanderPlas, Alexandre Passos, David Cournapeau, Matthieu Brucher, Matthieu Perrot, and Edouard Duchesnay. 2011. Scikit-learn: Machine Learning in Python. *JMLR* 12 (2011), 2825–2830.
- [48] Kexin Pei, Yinzhi Cao, Junfeng Yang, and Suman Jana. 2017. DeepXplore: Automated Whitebox Testing of Deep Learning Systems. In *SOSP*. ACM, 1–18.
- [49] J. Ross Quinlan. 1986. Induction of Decision Trees. *Machine Learning* 1 (1986), 81–106. Issue 1.
- [50] Kevin Roth, Yannic Kilcher, and Thomas Hofmann. 2019. The Odds Are Odd: A Statistical Test for Detecting Adversarial Examples. In *ICML (PMLR)*, Vol. 97. PMLR, 5498–5507.
- [51] Robert E. Schapire. 1999. A Brief Introduction to Boosting. In *IJCAI*. Morgan Kaufmann, 1401–1406.
- [52] Koushik Sen, Darko Marinov, and Gul Agha. 2005. CUTE: A Concolic Unit Testing Engine for C. In *ESEC/FSE*. ACM, 263–272.
- [53] Yash Sharma and Pin-Yu Chen. 2018. Bypassing Feature Squeezing by Increasing Adversary Strength. *CoRR* abs/1803.09868 (2018).
- [54] Janet Siegmund, Norbert Siegmund, and Sven Apel. 2015. Views on Internal and External Validity in Empirical Software Engineering. In *ICSE*. IEEE Computer Society, 9–19.
- [55] Youcheng Sun, Xiaowei Huang, and Daniel Kroening. 2018. Testing Deep Neural Networks. *CoRR* abs/1803.04792 (2018).
- [56] Youcheng Sun, Min Wu, Wenjie Ruan, Xiaowei Huang, Marta Kwiatkowska, and Daniel Kroening. 2018. Concolic Testing for Deep Neural Networks. In *ASE*. ACM, 109–119.
- [57] Christian Szegedy, Vincent Vanhoucke, Sergey Ioffe, Jonathon Shlens, and Zbigniew Wojna. 2016. Rethinking the Inception Architecture for Computer Vision. In *CVPR*. IEEE Computer Society, 2818–2826.
- [58] Christian Szegedy, Wojciech Zaremba, Ilya Sutskever, Joan Bruna, Dumitru Erhan, Ian J. Goodfellow, and Rob Fergus. 2014. Intriguing Properties of Neural Networks. In *ICLR*.
- [59] Yuchi Tian, Kexin Pei, Suman Jana, and Baishakhi Ray. 2018. DeepTest: Automated Testing of Deep-Neural-Network-Driven Autonomous Cars. In *ICSE*. ACM, 303–314.
- [60] Jingyi Wang, Guoliang Dong, Jun Sun, Xinyu Wang, and Peixin Zhang. 2019. Adversarial Sample Detection for Deep Neural Network Through Model Mutation Testing. In *ICSE*. IEEE Computer Society/ACM, 1245–1256.
- [61] Xiaofei Xie, Lei Ma, Felix Juefei-Xu, Minhui Xue, Hongxu Chen, Yang Liu, Jianjun Zhao, Bo Li, Jianxiong Yin, and Simon See. 2019. DeepHunter: A Coverage-Guided Fuzz Testing Framework for Deep Neural Networks. In *ISSTA*. ACM, 146–157.
- [62] Weilin Xu, David Evans, and Yanjun Qi. 2018. Feature Squeezing: Detecting Adversarial Examples in Deep Neural Networks. In *NDSS*. The Internet Society.
- [63] Valentina Zantedeschi, Maria-Irina Nicolae, and Amrith Rawat. 2017. Efficient Defenses Against Adversarial Attacks. In *AISeC@CCS*. ACM, 39–49.
- [64] Mengshi Zhang, Yuqun Zhang, Lingming Zhang, Cong Liu, and Sarfraz Khurshid. 2018. DeepRoad: GAN-Based Metamorphic Testing and Input Validation Framework for Autonomous Driving Systems. In *ASE*. ACM, 132–142.